Scheduling-based Transmit Signal Shaping in Energy-Constrained Molecular Communications

Mustafa Can Gursoy and Urbashi Mitra

Department of Electrical and Computer Engineering, University of Southern California, Los Angeles, CA, USA E-mails: {mgursoy, ubli}@usc.edu

Abstract—Diffusion-based molecular communications (DBMC) systems rely on diffusive propagation of molecules to convey information. In a DBMC system, as each emitted molecule experiences a stochastic delay, pulse shaping is crucial for a DBMC system's reliability and overall performance. To this end, acknowledging the inherent resource-limited nature of a DBMC system, a novel framework to model and optimize a DBMC transmitter is introduced in this paper. Leveraging tools from wireless packet scheduling theory, the DBMC pulse shaping problem is formulated as an energy-constrained resource allocation problem. Through the developed framework, it is shown that the provably optimal pulse shape that minimizes the error probability is the delayed-spike pulse, where the incurred delay is a decreasing function of the available energy budget. The framework is then extended to both absorbing and passive/observing receiver structures, as well as systems where molecules can degrade in the transmitter body prior to release. Numerical results corroborate the developed analysis, and show that the delayedspike outperforms conventional, non-zero-width pulse shapes in terms of error performance.

I. INTRODUCTION

Diffusion-based molecular communication (DBMC) is a way of conveying information through the exchange of chemical signals (molecules). A DBMC system relies primarily on diffusive propagation of the messenger molecules after their release, which causes each molecule to exhibit Brownian motion in the communication environment [1]. The randomness of Brownian motion introduces an inherent stochasticity to a DBMC system, and leads to molecules within a same transmission experiencing different delays in their arrivals at the receiver. The randomness can also lead to some molecules to never arrive at the receiver, causing significant attenuation in the received signal. Understanding and alleviating the effects of this stochasticity has lead to significant efforts into many subfields of DBMC research, such as channel modeling, modulation design, detection and equalization, source and channel coding, etc.

In a DBMC system, the received signal is significantly affected by the particular molecular waveform emitted by the transmitter (*i.e.*, the molecules' release times). Consequently, alongside modulation techniques, coding, and detection strategies, the performance of a DBMC system is also a function of the particular pulse shape employed by the transmitter. In [2], it is demonstrated that the best DBMC pulse shape

This work is funded in part by one or more of the following grants: NSF CCF-1817200, ARO W911NF1910269, DOE DE-SC0021417, Swedish Research Council 2018-04359, NSF CCF-2008927, NSF CCF-2200221, ONR 503400-78050, ONR N00014-15-1-2550, and the USC + Amazon Center on Secure and Trusted Machine Learning.

is a Dirac-delta at t = 0 (the earliest allowable emission time), in terms of minimizing the received signal spread at the receiver. In [3], the error performance of a DBMC system is considered for more practical pulse shapes such as square and exponential waves, and it is argued that while transmitting the same number of molecules, the exponential wave is typically a better alternative than square pulses. In [4]-[6], the use of multiple molecule types have been considered to induce a shorter pulse width at the receiver, through mathematical combining strategies [4], [5], or inducing chemical reactions in the channel [6]. In [7], it is shown that a similar received signal narrowing can also be induced by external enhancements of the DBMC channel, whereas [8], [9] show the received pulse can be narrowed through time differentiation at the receiver end. In [10], [11], adaptively changing the transmission rate over consequent symbols is considered, which can be considered as a frame-level shaping of the signal emitted by the transmitter. In [12], implementational aspects of pulse shaping is discussed in the context of microfluidic devices.

A DBMC system is inherently energy-limited, whether it be natural or synthetic. For example, devices in the nanoscale can face severe energy constraints [13], and microbial communities often avoid signal over-production to limit energy over-consumption and metabolic burden [14]-[16]. Furthermore, the messenger molecules are often converted from other molecules through chemical means prior to their release, particularly in DBMC systems that leverage microbial communities [17]–[19]. However, to the best of our knowledge, the problem of DBMC transmit pulse shaping has not yet been formally considered under energy-constraints on generating and releasing the messenger molecules, including aforementioned prior art. Motivated by this, we address energy-constrained DBMC pulse shaping herein. In particular, leveraging tools from wireless packet scheduling theory [20]-[23], we develop a theoretical framework that models a DBMC transmitter as a molecule-scheduling entity, which allows for formulating DBMC pulse shaping problems as resource (energy) allocation optimizations. Through this framework, we find the energyconstrained optimal pulse shapes for DBMC systems with varying receiver structures, transmitter constraints, as well as molecular degradation [24], [25].

In our previous works [22], [23], we developed a theoretical framework to model wireless packet transmission scheduling scenarios under *two-sided delay constraints*, which refers to scenarios where transmitting packets both too early and too late are undesirable. This also applies to DBMC systems; we explicitly map these delay constraints' correspondence to

2

- We develop a theoretical framework that fundamentally links pulse shaping and resource allocation for a DBMC system.
- 2) Using the developed framework, we solve the energy-constrained pulse shaping problem for a DBMC system. In particular, we provably show that the optimal pulse shape that minimizes the error probability for a DBMC system is the *delayed-spike*, whose incurred delay is a decreasing function of the available energy budget.
- We expand our framework to cover molecular degradation within the transmitter prior to signal emission, and provide pulse shaping strategies under said signal loss at the transmitter.
- 4) Numerical results support the analytical findings of the paper, and demonstrate that the delayed-spike outperforms the widespread non-zero-width pulse shapes such as the square and exponential waves.
- 5) The findings of the work can be flexibly utilized (or extended) to cover passive/observing receiver structures, different channel topologies, and molecular degradation profiles.

The remainder of the paper is organized as follows: Section II presents the system model and describes the problem of interest in the paper. Section III provides some key definitions and highlights the parallelisms between DBMC pulse shaping and scheduling theory. Section IV formally formulates the problems of interest, and solves for a special case to build intuition. Section V presents the main results, Theorems 1-2, which address error-optimal DBMC pulse shaping under energy constraints (and vice versa). The corresponding proofs are in Appendices B-C. Section VII provides extensions to the developed framework, mainly for i) cases where molecular degradation can occur within the transmitter prior to signal emission, and ii) passive receivers. Lastly, Section VIII concludes the paper.

II. SYSTEM MODEL

In this paper, unless stated otherwise, we consider a point-to-point DBMC system between a transmitter (TX) and an absorbing receiver (RX) in a one dimensional driftless channel. The distance between TX and RX is denoted by d, and the diffusion coefficient of the released messenger molecules (type-M) is denoted by D.

A. The Transmitter

In this paper, we consider a binary communication scenario, in which the transmitter employs a binary concentration shift

keying (BCSK) modulation to convey a single bit of information to the receiver by releasing N molecules for transmitting a bit b=1, and staying silent for b=0. We first emphasize that the methods developed in this paper can be extended to many other modulation schemes as well. We focus on BCSK due to its widespread use in the MC literature and its simple implementation by nano-scale machinery ([26]-[29], etc.). That said, expanding the typical considerations of said prior art, we herein consider an additional step in molecule release. In particular, as the messenger molecules are often converted/synthesized from other molecules prior to their release, we consider the case where the type-M messenger molecules need to be synthesized prior to their release towards the receiver. For a BCSK bit-1 transmission, N number of type-M molecules are converted from type-S source molecules through some chemical reaction chain that yields $S \to M$, which takes a certain duration τ_i and incurs an energy consumption/metabolic burden cost $w(\tau_i)$. Defining $\tau = |\tau_1 \cdots \tau_N|$, we assume the cost associated with converting/processing and releasing all N molecules to have the following properties:

- 1) The overall cost incurred by the whole transmission is decomposable in each $w(\tau_i)$, that is $w(\tau) = \sum_{i=1}^{N} w(\tau_i)$.
- 2) For a particular argument τ_i , $w(\tau_i)$ is strictly convex and decreasing in τ_i , and is positive $(w(\tau_i) > 0$ for all i).
- 3) Given τ_i , $w(\tau_i)$ does not depend on time index *i*. That is, each molecule is indistinguishable/identical.

We assume there are sufficiently many type-S molecules at the transmitter at t=0 to convert to type-M messenger molecules. Also note that the case for bit-0 is trivial from a pulse shaping standpoint as no molecules are released.

We note that for a single, individual chemical reaction, the activation energy required to achieve it implies a constant energy cost w, regardless of τ . However, looking at the aggregate behavior of an MC node (e.g., a bacterial cell), a faster production rate of a certain MC signaling molecule (i.e., smaller τ values) would incur increasingly higher metabolic burden in the cell [30]–[33]. The convex-decreasing nature of $w(\tau)$ is inspired from this relationship, and represents the dramatic metabolic burden increase of rapidly producing signaling molecules. The extension of our framework to other, non-convex $w(\tau)$ functions is an interesting future research direction. Throughout the remainder of the paper, we will use the words energy and cost interchangeably, both referring to $w(\tau)$.

B. The Channel

After a molecule is released from TX, it can undergo a degradation reaction in the communication channel, which renders it unusable from a communication perspective at RX. Molecular degradation is commonly modeled as a first-order reaction hence an exponential decay profile in the MC literature ([24], [25], [34], etc.), which we also employ herein. Subject to exponential decay, a molecule's degradation-induced lifetime is an exponentially distributed random vari-

able with rate k, which implies that its survival probability until a particular time t after its release to be [24]

$$p_{\text{surv}} = P(T_{\text{surv}} > t) = e^{-kt},$$

where $T_{\rm surv}$ denotes said degradation-induced lifetime. Overall, for a 1-D driftless DBMC channel with exponential degradation, a molecule's arrival time density, $f_{hit}(t)$, is given by [34]

$$f_{hit}(t) = \frac{d}{\sqrt{4\pi Dt^3}} \exp\left(-\frac{d^2}{4Dt} - kt\right). \tag{1}$$

Equation (1) implicitly assumes a molecule's release time is $\mathcal{T}_i = 0$. The case where $\mathcal{T}_i > 0$ simply shifts the support of $f_{hit}(t)$ to the right by \mathcal{T}_i .

C. The Receiver

At the receiver end, the receiver collects the type-M molecules as they arrive, and increments its received molecule counter by one upon each arrival. The receiver collects the molecules within a symbol duration defined by the interval $[0,t_R]$, and obtains the arrival count y. The receiver then performs a threshold detection with threshold γ to decode the BCSK symbol by performing

$$y \underset{H_0}{\gtrless} \gamma, \tag{2}$$

where H_i denotes the hypothesis that bit-i was transmitted. Note that for our theoretical analysis in Sections IV-V, we consider a one-shot communication scenario where only a single bit is sent (*i.e.*, a no-ISI scenario). A one-shot model is accurate in the lower data rate regime, wherein ISI is negligible due to diffusion dynamics (see [35]–[37], etc.). A rigorous extension to with-ISI scenarios is a non-trivial one, and we pose this problem as a future research question. That said, although rigorous theoretical analysis is given for no-ISI systems, the proposed pulse shape explicitly mitigates the effects of ISI as well. Numerical results we provide in Section VI do consider ISI in their evaluations, and confirm the efficacy of the proposed scheme in with-ISI systems.

In the one-shot BCSK transmission scenario considered, a molecule with index i and a particular release time \mathcal{T}_i has until t_R to successfully arrive at the receiver (while also surviving until its arrival). Denoting this success probability as p_i , following from (1), we have

$$p_{i}(\mathcal{T}_{i}) = \int_{0}^{t_{R} - \mathcal{T}_{i}} f_{hit}(t)dt$$

$$= \frac{1}{2}e^{-\sqrt{\frac{k}{D}}d}\operatorname{erfc}\left[\frac{d}{\sqrt{4D(t_{R} - \mathcal{T}_{i})}} - \sqrt{k(t_{R} - \mathcal{T}_{i})}\right]$$

$$+ \frac{1}{2}e^{\sqrt{\frac{k}{D}}d}\operatorname{erfc}\left[\frac{d}{\sqrt{4D(t_{R} - \mathcal{T}_{i})}} + \sqrt{k(t_{R} - \mathcal{T}_{i})}\right],$$
(3)

where $\operatorname{erfc}(\cdot)$ is the Gaussian complementary error function.

We note that although the framework in this paper is presented through its application on a 1-D driftless system, the cases for three dimensional diffusion channels follow almost identically to the 1-D case we consider herein: the only difference arises from the particular arrival density function $f_{hit}(t)$ and its integral that defines the successful arrival probability. The solutions as well as the approach developed in this paper thus can be directly adapted to 3-D systems, as well as other cases with other arrival density functions (e.g., DBMC systems with flow).

III. PRELIMINARIES

As previously mentioned, the transmitter's goal is converting N type-S molecules to type-M messenger molecules, and releasing them towards the receiver to transmit a bit-1 to the DBMC receiver. In this section, we provide a methodical novel framework of optimizing MC transmission, leveraging concepts and approaches from wireless packet scheduling theory [20]–[22]. In particular, we first address minimizing energy consumption/metabolic burden of an MC transmitter via arranging molecule processing durations (*i.e.*, τ_i), subject to constraints on communication fidelity (*i.e.*, bit-error ratio, BER). Leveraging this result, we then address the dual formulation, perhaps of more interest, which seeks to minimize BER subject to constraints on the available energy budget at the transmitter.

For a molecule to be successfully counted towards the received signal at the RX, it needs to i) successfully arrive at the receiver, and ii) survive until the molecule has arrived. Clearly, a molecule has a higher probability of arrival if it has more time to arrive at the receiver, thus the first condition implies the molecule should depart the transmitter as soon as possible. Likening this phenomenon to our nomenclature from our prior works [22], [23], we call this diffusion-delay induced need for earlier transmission the *pre-transmission delay (pre-delay) constraint*. Note that a pre-delay constraint constrains time block available prior to release, and implies "earlier release the better".

On the other hand, the more time a molecule requires for absorption, the longer it needs to survive. Thus, from a purely molecule survival perspective, a later release is better, which we call a *post-transmission delay (post-delay) constraint*. These two factors (diffusive delay and molecular degradation) compete and the govern appropriate time of release of a molecule to maximize its probability of successful reception (that is, p_i) within the symbol duration. We note that which of these factors dominate is highly dependent on the receiver structure. For example, in this paper's system of interest (absorbing receivers that increment their arrivals upon molecule reception), p_i is a decreasing function of the release time \mathcal{T}_i (see Figure 1 for visualization). We will leverage this monotonic behavior when optimizing the MC transceivers.

In Subsection VII-B, we discuss an extension to the presented framework of this paper to passive receivers [37], instead of absorbing ones that we typically consider throughout the paper. For passive receivers that sample at t_R to obtain y, we will observe that diffusive propagation (pre-delay) and molecule lifetime (post-delay) can in fact conflict, which can break the monotonicity of p_i in \mathcal{T}_i . The behavior of p_i is governed by the relationship between d, D, k, and t_R .

Fig. 1. Successful reception probability p_i with respect to \mathcal{T}_i for a 1-D DBMC system with molecular degradation. $d=10\,\mu\mathrm{m},\ D=100\,\mu\mathrm{m}^2\,\mathrm{s}^{-1},\ k=1\times10^{-3}\,\mathrm{s}^{-1},\ t_R=10\,\mathrm{s}.$

IV. ARRANGING PROCESSING DURATIONS: THE ONE-BY-ONE PROCESSING CASE

In our prior works [22], [23], we showed that in cases where all propagation delays obey $t_{\text{prop},i} < t_R$, and the transmitter has access to the propagation delay and degradation-induced lifetimes of each molecule a priori, it can arrange the molecule departure times \mathcal{T}_i such that the arrival of all N molecules are guaranteed. This is valid for configurations where either preand post-delay constraints are present, or possibly both. However, the DBMC setup is inherently subject to stochasticity in propagation delays due to the Brownian motion exhibited by the type-M molecules after their release [38]. Even further, a molecule can randomly degrade in the channel, which adds another degree of stochasticity to the received signal at the receiver end [24], [25]. Due to this inherent randomness, the arrival of all N molecules can never be guaranteed with full certainty, as there can always be a particularly long diffusive delay of a molecule, or an extremely fast degradation. To this end, we take a stochastic approach herein.

A. Error-Constrained Energy Minimization

Either engineered biological systems or synthetic human-made devices, DBMC transceivers are envisioned to be employed in small-scale operations, thus managing their metabolic burden and/or their energy efficiency is crucial for their operation and longevity [13]. On the other hand, achieving better communication fidelity via providing low error rates is a hallmark of success in any form of communication technology, including DBMC systems. Motivated by this, this section first proposes a scheduling-based DBMC pulse shaping design that tackles energy consumption $w(\tau)$. Afterwards, Subsection IV-B will leverage the results and the intuition built in this subsection to optimize the pulse shape to minimize error rates.

Firstly, leveraging our prior approach developed in [23], we address the energy consumption optimization problem. In particular, we herein seek to minimize the transmitter's $w(\tau)$ while converting and releasing the N molecules for a BCSK bit-1, subject to satisfying a target error probability $P_{\rm target}$ as

a quality of service measure. In its most general form, the overall problem can be formulated as

$$\min_{\tau} w(\tau) = \sum_{i=1}^{N} w(\tau_i)$$
 (4a)

s.t.
$$P_e(\boldsymbol{\tau}; \gamma, d, D, k, t_R) \le P_{\text{target}}$$
 (4b)

$$0 < \tau_i < t_R, \quad \forall i = 1, \dots, N. \tag{4c}$$

Note that the error probability, denoted by P_e , is a function of the duration times τ , as τ_i 's affect each molecule's release time \mathcal{T}_i . Recall that the integral in (3) is maximized for a fixed t_R when $t_R - \mathcal{T}_i$ is minimized. An error event for a bit-1 transmission occurs when $y < \gamma$, thus having a smaller τ_i (thus smaller \mathcal{T}_i) implies a smaller error probability. In fact, to minimize P_e , each molecule should ideally have as much time between their release and t_R to maximize their capture probability, leading to the error-minimizing release time vector $\mathcal{T} = \mathbf{0}$, implying $\boldsymbol{\tau} = \mathbf{0}$. However, this incurs a large cost $w(\tau)$, as $w(\tau)$ is convex and decreasing in τ . On the other hand, a larger set of τ_i 's would alleviate this, but would decrease arrival probabilities and increase errors. In essence, for a one-shot BCSK transmission, there is a fundamental trade-off between energy consumption and error probability, leading to the constrained optimization problem in (4).

First-in First-out Ordering: To build intuition into the design strategy, we first address the case where the transmitter synthesizes each type-M molecule from its type-S source molecule one-by-one (while other type-S molecules wait in a queue to be processed). The transmitter waits until it synthesizes all N messenger molecules for transmitting b=1, and releases them together at the time of completion. Note that this implies $\mathcal{T}_i = \sum_{j=1}^N \tau_j$ for all i. Let $\tau_r = \sum_{j=1}^N \tau_j = \mathcal{T}_i$ denote this common release time.

As each molecule departs at the same time, each molecule observes an equal $p_i(\tau_r)$. Thus, the total arrival count at the receiver until time t_R , denotes by y, follows a binomial distribution with N trials and success probability $p_i(\sum_{j=1}^N \tau_j)$ obtained from (3). Assuming equally likely bit transmissions, and observing that P(error|b=0)=0 under no ISI and external noise, the theoretical error probability for the one-shot BCSK system with a decision threshold γ can then be expressed as

$$P_{e} = \frac{1}{2}P(\text{error}|b=0) + \frac{1}{2}P(\text{error}|b=1) = \frac{1}{2}P(y < \gamma)$$

$$= \frac{1}{2}\text{CDF}^{(\mathcal{B})}(\lfloor \gamma \rfloor; N, p_{i}(\tau_{r}))$$

$$= \frac{1}{2}I_{1-p_{i}(\tau_{r})}(N - \lfloor \gamma \rfloor, \lfloor \gamma \rfloor + 1).$$
(5)

Here, ${\rm CDF}^{(\mathcal{B})}(x;n,p)$ denotes the binomial cumulative distribution function (CDF) evaluated at x, and $I_x(a,b)$ denotes the regularized incomplete Beta function with $I_x(a,b)=\frac{\int_0^x u^{a-1}(1-u)^{b-1}du}{\int_0^1 u^{a-1}(1-u)^{b-1}du}.$

¹In wireless packet scheduling literature, this ordering is commonly referred to as the first-in first-out (FIFO) rule ([20]–[22], *etc.*).

Recall that the error probability P_e is monotone increasing in τ_r , whereas $w(\tau_i)$ is monotone decreasing. Then, the optimal τ_r for the error-constrained energy minimization problem in (4) for FIFO ordering simply becomes the largest τ_r that critically satisfies the target error probability

$$\tau_r = \{ \tau \mid I_{1-p_i(\tau)}(N - \lfloor \gamma \rfloor, \lfloor \gamma \rfloor + 1) = P_{\text{target}} \}. \tag{6}$$

The set is guaranteed to have a single element due to the monotonicity of P_e in τ_r , thus the solution for the release time in the FIFO case is unique.

The question of allocating individual τ_i 's for a given τ_r remains. To solve this problem, we first highlight that as a direct consequence of its definition in Subsection II-A, $w(\tau)$ is a Schur-convex function². Under a Schur-convex cost function w(x), if a vector x_1 gets majorized by another vector x_2 (i.e., is more "balanced", see footnote 3 and [21], [22], [39]), this necessarily implies that $w(x_1) < w(x_2)$.³ Thus, given a particular τ_r , the optimal solution that minimizes $w(\tau)$ is the τ vector that gets majorized by any other N-element duration vector that sums up to τ_r . This vector is simply the vector of equal elements. Thus, given said common release time τ_r that is found by solving (6), the most cost-efficient allocation among individual τ_i 's is setting $\tau_i = \frac{\tau_r}{N}$ for all i, which solves the problem when combined with (6).

An interesting observation is that the energy-optimal solution is not dependent on the particular form of the $w(\tau)$ function. As long as it is convex and decreasing, and the properties laid out in Subsection II-A are satisfied, the solution that finds τ_r by (6) and sets $\tau_i = \frac{\tau_r}{N}$ is always optimal.

B. Energy-Constrained Pulse Shaping for Error Probability Minimization

As a "dual" to the error-constrained energy efficiency problem, the problem of minimizing the error probability with a fixed energy budget can also be of particular interest in data communication applications of DBMC. Leveraging the solution strategy we previously determined, we address this new problem herein. Similar to Subsection IV-A, we also consider each molecule to be processed/converted one-by-one, stored until the whole batch of N molecules is complete (at time τ_r), and released at $\mathcal{T}_i = \tau_r$ (i.e., the FIFO case). Denoting $w_{\rm max}$ as the available total energy budget, (7) describes the corresponding problem:

$$\min_{\boldsymbol{\tau}} \quad P_e(\boldsymbol{\tau}; \gamma, d, D, k, t_R) \tag{7a}$$

s.t.
$$w(\tau) = \sum_{i=1}^{N} w(\tau_i) = w_{\text{max}}$$
 (7b)

$$0 < \tau_i < t_R, \quad \forall i = 1, \dots, N. \tag{7c}$$

Similar to Subsection IV-A, we leverage the monotonicity of P_e in τ_r to find an analytical solution for the optimal τ vector.

In particular, we again note that P_e is minimized if and only if τ_r is minimized, which implies that the error minimization problem is in fact equivalent to minimizing $\tau_r = \sum_{i=1}^N \tau_i$. Thus, this finding shows us that the energy-constrained error minimization problem in DBMC with FIFO processing is fundamentally analogous to the so-called *completion time minimization* problem in wireless packet scheduling [41], [42], which we had addressed in our prior work [23], whose tools we leverage herein.

In our earlier work, through Lemmas 4 and 5 of [23], we had shown that the necessary and sufficient conditions when minimizing completion time are the following:

- The allocation vector au exhausts all of the available $w_{\rm max}$ budget when allocating.
- The vector $\pmb{\tau}$ is energy-optimal within the interval $[0,\sum_{i=1}^N \tau_i]$.⁴

For this subsection's case of interest, combining these two conditions, the minimum attainable completion time is attained when $\tau_i = w^{-1}(\frac{w_{\max}}{N})$ for all i, since this allocation both exhausts w_{\max} and ensures energy-optimality (equal allocation is the best allocation due to majorization, see Subsection IV-A). Thus, the earliest release time is $\tau_r = Nw^{-1}(\frac{w_{\max}}{N})$. It then follows from the monotonicity of P_e that the minimum attainable error probability with a budget of w_{\max} is

$$P_e^* = I_{1-p_i(Nw^{-1}(\frac{w_{\text{max}}}{N})}(N - \lfloor \gamma \rfloor, \lfloor \gamma \rfloor + 1).$$
 (8)

Note that similar to the energy-minimization problem, the optimal allocation for energy-constrained error minimization also entails balancing as much as possible. Furthermore, this approach is again independent of the particular $w(\tau)$ function, as long as it is convex and decreasing in τ , and τ_i are interchangeable (thus Schur-convex). That said, the actual value attained by the optimal allocation can change according to the particular $w(\tau)$ function and system parameters d, D, k, and t_B .

V. SIMULTANEOUS SYNTHESIS OF SIGNAL MOLECULES: DBMC PULSE SHAPE OPTIMIZATION

The one-by-one processing consideration is akin to a queue with a single server in queueing theory [43], which finds MC examples in confined tunnels of cascaded enzymatic reactions (mentioned as substrate channeling in [44]). However, it is likely that in many MC systems, messenger molecules are synthesized simultaneously (e.g., through different enzyme molecules or independent, spontaneous reactions [45]). Motivated by this, in this section, we remodel the system in Section IV to allow for simultaneous production of different molecules. In particular, we consider each of the N molecules to be independently synthesized, taking τ_i duration for its $S \to M$ conversion, and released as it is synthesized (that is, $\mathcal{T}_i = \tau_i$).

We first highlight that a set of molecule release times, \mathcal{T} , is akin to a pulse shape in DBMC [2], [3]. For example, a set of equally spaced molecule releases is equivalent to a square pulse; an instantaneous release of N molecules represents

⁴Condition 1 follows from $w(\tau)$ being decreasing, and Condition 2 follows from a contradiction on Condition 1. For further details, see [23].

 $^{^2}$ A function is Schur-convex if it is defined on a symmetric convex set A, is symmetric with respect to variable permutations, and it is a convex function of its variables [39], [40]. The considered $w(\tau)$ satisfies all three of these requirements.

 $^{^3}$ An N-element, non-increasing sequence \boldsymbol{x}_1 is said to be majorized by another N-element, non-increasing sequence \boldsymbol{x}_2 if summing up to the same value, $\sum_{i=1}^N x_{1,i} \leq \sum_{i=1}^N x_{2,i}$ holds for all $m=1,\ldots,N-1$.

a spike, etc. Acknowledging this, and recalling $\mathcal{T}_i = \tau_i$, it follows that arranging the τ vector is equivalent designing a pulse shape. In the remainder of the section, we will use τ -optimization and pulse shaping interchangeably.

A. Pulse Shaping for Error-Constrained Energy Minimization

Following a similar order to the FIFO case, we first address pulse shaping for energy minimization subject to a target error probability (Equation (4)), $P_{\rm target}$, for this newly considered arbitrary release time case. We will then follow by addressing the dual problem (Equation (7)), that is, energy-constrained BER minimization.

Prior to providing a solution, we first observe that contrary to Section IV, each molecule can potentially depart at different times in this section. Thus, we can now potentially have $p_i(\tau_i) \neq p_j(\tau_j)$ for $i \neq j$, and the exact error probability can no longer be evaluated by the binomial CDF due to unequal success probabilities. In particular, denoting $p_i(\tau_i) = p_i$ for brevity, the sum of N independent Bernoulli random variables with success probabilities p_1, \ldots, p_N follow a Poisson-binomial distribution, with probability mass function (PMF)

$$P(y=k) = \sum_{A \in \mathcal{S}_k} \prod_{i \in A} p_i \prod_{j \notin A} (1 - p_j), \qquad (9)$$

where \mathcal{S}_k is the set of all k-element subsets of the N-element set of molecules, and A is an arbitrary element of \mathcal{S}_k . Thus, given γ and a particular τ vector with induced successful arrival probabilities $p_i = p_i(\tau_i)$, the error probability for threshold-decoded BCSK can be expressed as

$$P_{e} = \frac{1}{2}P(y > \gamma|b = 0) + \frac{1}{2}P(y \le \gamma|b = 1) = \frac{1}{2}P(y < \gamma)$$
$$= \frac{1}{2}\sum_{k=0}^{\lfloor \gamma \rfloor} \sum_{A \in \mathcal{S}_{k}} \prod_{i \in A} p_{i} \prod_{j \notin A} (1 - p_{j}).$$
(10)

We now present Theorem 1, which provides the energy-optimal pulse shape for BCSK signaling. Specifically, Theorem 1 states that the optimal solution has all τ_i equal, and critically meets the target error probability.

Theorem 1. In a single-shot diffusive MC system using BCSK signaling with threshold detection, under a convex decreasing energy cost of molecule production duration, given $\tau_i < t_R - \frac{\sqrt{9+\frac{4kd^2}{D}}-3}{4k}$ is satisfied, the energy-minimizing τ vector has $\tau_i = \{\tau \mid I_{1-p_i(\tau_i)}(N-\lfloor \gamma \rfloor, \lfloor \gamma \rfloor + 1) = P_{\mathrm{target}}\}$ for all $i=1,\ldots,N$. That is, $P_e(\tau) = P_{\mathrm{target}}$, and $\tau_i = \tau_j$ for all i,j.

Overall, Theorem 1 shows that in a single-shot DBMC system using BCSK with threshold detection, the (uniquely) optimal pulse shape in terms of error-constrained energy-minimization is a *delayed spike*. Furthermore, the optimal τ_i values can simply be found by critically satisfying the target error probability. Note that for all τ_i equal, the error probability expression in (10) becomes equivalent to (5).

Theorem 1 is valid when the system is operating in a regime where τ_i is "small" $(\tau_i < t_R - \frac{\sqrt{9 + \frac{4kd^2}{D} - 3}}{2k})$. This is an added constraint with respect to FIFO (which allows for all $\tau_i < t_R$), and ensures the error probability is Schur-convex in τ_i (which is leveraged in the optimality proof in Appendix B). For further details, we refer the reader to Lemma 1 in Appendix A. Note that having a small τ_i regime also corresponds to yielding low error probability, which is typically the desired operating regime of a DBMC system, softening the added τ_i constraint's restrictiveness. The inflection point at $\tau_i=t_R-\frac{\sqrt{9+\frac{4kd^2}{D}-3}}{4k}$ is dependent on the relationship between d,D,t_R , and the decay rate k. It holds irrespective of the decision threshold γ , and p_i values other than the one of interest (p_i) . In Figure 2, we present an example with N=3 molecules to corroborate the proof in Appendix A, and our discussion herein. The figure presents the error probability expression provided in (10) and this inflection point. For demonstrative purposes, the plots consider fixed p_2 and p_3 values and sweeps P_e with respect

Figure 2 demonstrates that the inflection point is not significantly restricting the system at hand over a large range of parameters. It also supports the theoretical analysis in Appendix A that the smaller error rate regime (i.e, left hand side of the inflection point) indeed yields a convex P_e in τ_i . Throughout the remainder of this paper, we assume that the system is operating in this low error probability/small τ_i regime.

Note that similar to the FIFO case, the solution strategy for optimal $\boldsymbol{\tau}$ vector found in Theorem 1 is not dependent on the particular $w(\tau)$ function. As long as $w(\tau)$ is convex and decreasing in its argument (τ) and $\tau_i < t_R - \frac{\sqrt{9 + \frac{4kd^2}{D} - 3}}{4k}$ is satisfied, the optimality of the fully balanced τ_i holds. That said, the actual value of the cost, $w(\boldsymbol{\tau})$, is clearly dependent on the specific $w(\tau)$ of the system.

B. Pulse Shaping for Energy-Constrained Error Minimization

As mentioned in Section IV-B, from a DBMC design perspective, minimizing the error probability with the available resources is of particular interest. To this end, we herein present the main result of the paper: The optimal pulse shape for BER minimization under a limited energy budget $w_{\rm max}$. In particular, we now extend the results of Theorem 1 to its dual problem of energy-constrained error minimization, through presenting Theorem 2.

We assume the problem is well-posed, that is, the available budget w_{\max} can provide a valid duration vector with $\tau_i < t_R - \frac{\sqrt{9 + \frac{4kd^2}{D}} - 3}{4k}$. Given a valid solution exists, by leveraging the duality between energy- and time-optimal scheduling, Theorem 2 finds the minimum attainable error probability of a threshold-decoded BCSK system under no ISI, given a certain budget w_{\max} .

Theorem 2. In a single-shot diffusive MC system using BCSK signaling with threshold detection, under a convex decreasing energy cost of molecule production duration $w(\tau)$ and a total energy budget $w_{\rm max}$, the error probability-minimizing duration

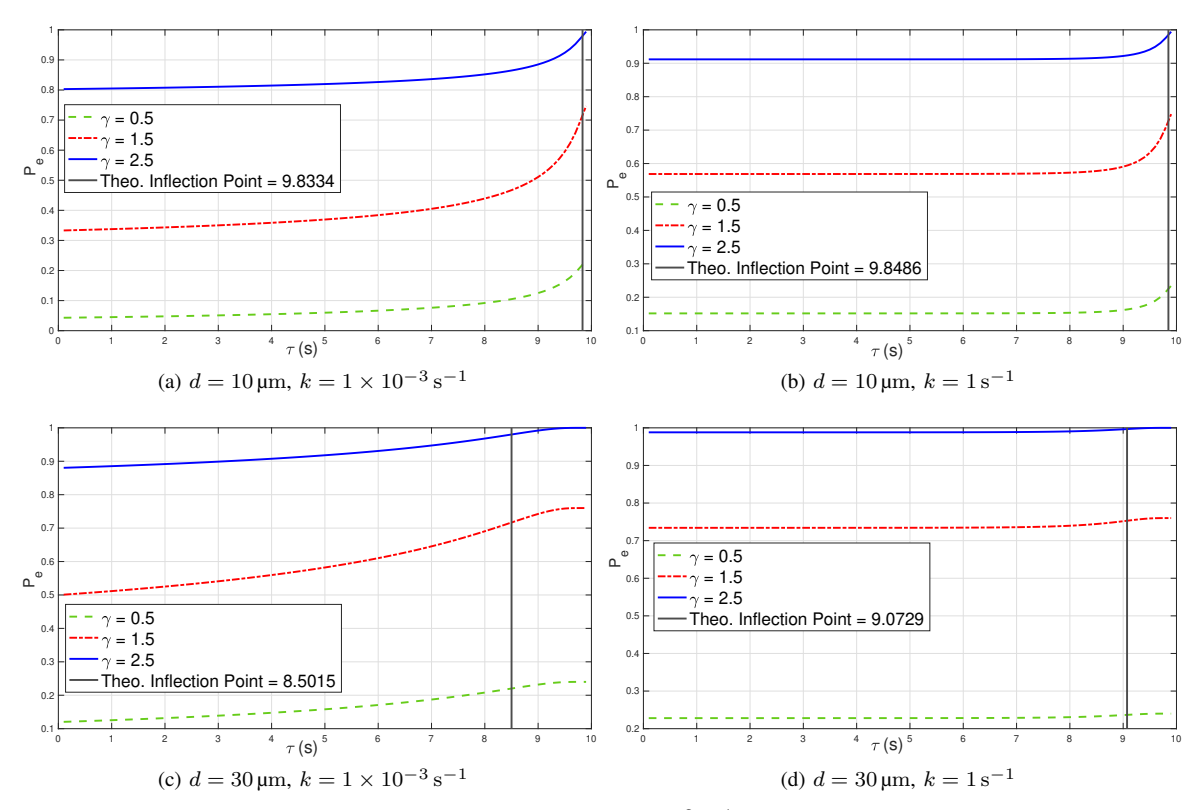


Fig. 2. Convexity of P_e in (10) with respect to τ_i . $p_2 = 0.4$, $p_3 = 0.6$, $D = 100 \, \mu \text{m}^2 \, \text{s}^{-1}$, and $t_R = 10 \, \text{s}$.

vector τ consists of $\tau_i = w^{-1}(\frac{w_{\text{max}}}{N})$ for all i = 1, ..., N. Thus, the lowest attainable error rate is

$$P_e^* = I_{1-p_i(w^{-1}(\frac{w_{\max}}{N})}(N-\lfloor\gamma\rfloor,\lfloor\gamma\rfloor+1).$$

The result of Theorem 2 shows that under a fixed energy budget and a convex cost, the uniquely optimal one-shot BCSK pulse is a delayed spike, with the optimal delay equal to $w^{-1}(\frac{w_{\max}}{N}).$ Note that as $w_{\max} \to \infty,$ the delay converges to $\tau_i \to 0.$ This is in agreement with prior results, which suggest that under no constraints, the optimal pulse is a delta at t=0. From this perspective, the delay of $\tau_i=w^{-1}(\frac{w_{\max}}{N})$ can be considered as the price of having a limited budget for transmission. To illustrate this point, Figure 3 presents the delay-budget curve (i.e., the τ_i -wmax curve) for $w(\tau)=\frac{1}{\tau}$ as a demonstrative example.

Similar to other results in Sections IV-Section V, for the error minimization case, as long as $w(\tau)$ is convex and decreasing in its argument (τ) and $\tau_i < t_R - \frac{\sqrt{9 + \frac{4kd^2}{D}} - 3}{4k}$, the solution form for optimal τ vector is the delayed spike. However, the actual value of the delay is clearly affected by the particular $w(\tau)$ of the system of interest.

VI. NUMERICAL RESULTS

In this section, we compare the theoretically optimal delayed-spike to conventionally considered pulse shapes with non-zero width under a fixed energy budget $w_{\rm max}$, in particular the square pulse considered in [2], [3] and the exponential

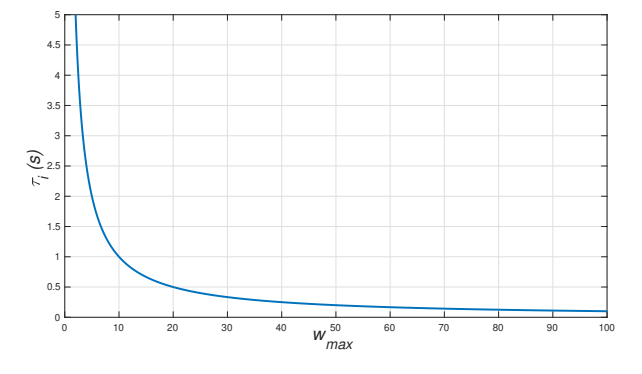


Fig. 3. The τ_i vs. w_{max} curve for $w(\tau) = \frac{1}{\tau}$, N = 10.

pulse [3]. Note that although we developed our theoretical analysis for single-shot (no-ISI) systems (*i.e.*, Sections IV-V), the numerical results in this section do consider ISI. The channel memory is selected as S = 10, which covers at least 99.9% of all successful molecule arrival probabilities for data points evaluated in the section. All data points are evaluated over 10^7 bit transmission realizations.

As detailed in Section V, the delayed-spike has release times $\mathcal{T}_i = w^{-1}(\frac{w_{\max}}{N})$ for all molecules to be transmitted. On the other hand, the non-zero width pulses with pulse width W_p reside within an interval $[t_{\text{begin}}, t_{\text{begin}} + W_p]$ for some pulse begin time t_{begin} . Note that each pulse shape has a different $w(\tau_i)$ distribution in the molecules, thus these pulse begin times can vary according to the strategy employed and W_p . For example, the square pulse has a constant rate of

Overall, the results in Figure 4 demonstrate that BER improves as the pulse width narrows. This supports the analysis in Section V, and corroborates the optimality argument of the delayed-spike (i.e., the zero-width pulse). Note that for non-zero-width pulses, while fully exhausting w_{max} , some release times are expected to be smaller than the delayedspike's common release time, whereas some are larger. These larger release times incur smaller p_i values compared to $p_i(w^{-1}(\frac{w_{\text{max}}}{N}))$, whereas smaller release times have larger p_i . Due to convexity of P_e and $w(\tau)$, the detriment of these larger \mathcal{T}_i outweigh the benefits of smaller release times, which leads to worse performance compared to fully balancing all \mathcal{T}_i (i.e., the delayed-spike). Note that this effect is more severe for smaller t_R as p_i values are more sensitive to increases in \mathcal{T}_i in this regime. As a result, the improvement of the delayed-spike over non-zero-width pulses is expected to be more pronounced when t_R is smaller. Note that the above explanation applies to systems both with and without ISI. In the presence of ISI, the detriment of having a larger \mathcal{T}_i is even more pronounced compared to the no-ISI case, as molecules that are released later are more likely to cause ISI to future symbols, in addition to having lower p_i for the intended symbol.

An interesting observation is that given a fixed $w_{\rm max}$, the error rate is not necessarily monotone-decreasing in N, which is unlike DBMC systems without any energy constraints. Note that as N increases, the available energy per molecule decreases (e.g, $\frac{w_{\rm max}}{N}$ for delayed-spike), which causes each molecule's release time $\mathcal{T}_i = \tau_i$ to increase. This decreases p_i and makes each molecule have a smaller probability of contributing to the received signal, which poses a trade-off with the benefits of increasing N (number of molecules N is also the number of trials of a Poisson-binomial for a no-ISI system, see (10)). As can also be observed from Figure 4b, the optimal N that minimizes BER is a function of the employed pulse shape and the pulse width W_p (in addition to system parameters such as $w_{\rm max}$, the cost function $w(\tau)$, and the channel parameters).

VII. EXTENSIONS

In this section, we discuss some extensions on the provided framework and the corresponding solution of Section

Algorithm 1 Error-minimizing pulse shaping under perfect type-S degradation, statistical type-M degradation and diffusion delay.

```
Inputs: N, w_{\text{max}}, w(\tau), t_R, k, d, D
 1: Initialize c = 0
 2: while 1 do
         Set \tau_i = T_{\text{deg},i} for all i = 1, \ldots, c
 3:
         Compute remaining energy:
         w_{\text{rem}} = w_{\text{max}} - \sum_{i=1}^c w(T_{\text{deg},i}) Allocate remaining durations equally:
         \tau_{c+1} = \cdots = \tau_N = \frac{w_{\text{rem}}}{N} if \tau_i \leq T_{\deg,i} for all i=1,\ldots,N then
 7:
 8:
         else
 9:
             c \leftarrow c + 1
10:
         end if
11: end while
      return 	au
```

V. Specifically, we address the pulse shaping optimization problem (for error minimization) under new added constraints and receiver structures.

A. Degradation within Transmitter

In the original problem formulation, we considered diffusive delay, as well as molecular degradation in the channel after molecules are processed and released. In this subsection, we extend our analysis to systems where molecules can also degrade within the transmitter body, prior to their conversion and release. We revisit the energy-constrained error-minimization problem in Subsection V-B under this added constraint.

Let $T_{deg,i}$ be the degradation-induced lifetime of a molecule within the transmitter body. That is, each type-S molecule degrades at $t=T_{deg,i}$, thus if $\tau_i>T_{deg,i}$, the molecule is lost before being converted to type-M and released⁵. Similar to the framework in Sections IV-V, the goal of the transmitter in this subsection is successfully converting all N type-S molecules (now before they degrade at $T_{deg,i}$), to minimize P_e subject to a fixed energy budget w_{\max} .

1) The Case with Full Lifetime Information: We first address the case where the transmitter has perfect a priori knowledge on these lifetimes $T_{deg,i}$. Note that information on diffusive propagation and type-M degradation in the channel are still only statistical. For this case, we provide Algorithm 1, which yields the error-minimizing τ vector (pulse shape) for the case where type-S lifetimes are perfectly known. Algorithm 1 assumes $T_{\deg,i}$ are ordered in a non-decreasing manner (i.e., $T_{\deg,1} \leq T_{\deg,2} \leq \cdots \leq T_{\deg,N}$) for convenience in presentation. Note that this assumption does not lose generality, as the molecules are identical/indistinguishable from a communication perspective (they contribute to y equally).

Algorithm 1 proposes that if type-S degradation times are perfectly known, the optimal solution algorithm resembles a water-filling strategy. Specifically, if the available $w_{\rm max}$ allows for having $\tau_1 = \cdots = \tau_N < T_{\rm deg,1}$, the optimal pulse shape is again a τ_i -delayed spike, which is in agreement with

 $^{^5 \}rm We$ assume this degradation can happen until the molecule's $M \to S$ is completed and the type-M molecule released.

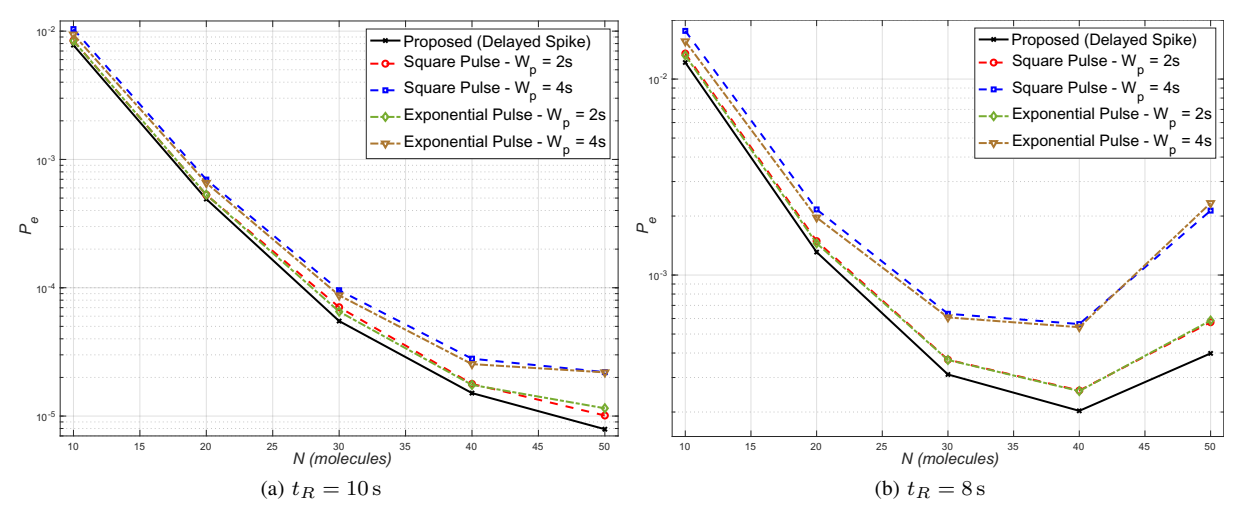


Fig. 4. BER vs. N for different pulse shapes. $w(\tau) = \frac{1}{\tau}$, $w_{\rm max} = 10$, $d = 10 \, \mu \rm m$, $D = 100 \, \mu \rm m^2 \, s^{-1}$, $k = 1 \times 10^{-3} \, \rm s^{-1}$, S = 10, $\gamma = \frac{N}{2} + 0.5$ for all data points.

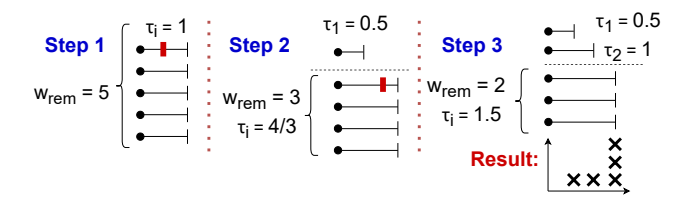


Fig. 5. An example for Algorithm 1 with $N=5, w_{\max}=5, w(\tau)=\frac{1}{\tau}, T_{\deg}=\left[0.5, 1, 1.8, 2, 2.7\right]$. The resultant vector $\boldsymbol{\tau}=\boldsymbol{\mathcal{T}}=\left[0.5, 1, 1.5, 1.5, 1.5\right]$.

Theorem (2). However, if the available $w_{\rm max}$ is too low for equal allocation, Algorithm 1 sets $au_1 = T_{{
m deg},1}$, and seeks to equalize $\{\tau_2 = \cdots = \tau_N\}$ with the remaining energy. The algorithm passes over the molecules one-by-one, and runs until it finds the smallest c such that $\tau_i = T_{{
m deg},i}$ for all $i \leq c$ and $\tau_{k+1} = \cdots = \tau_N$ are both satisfied with the available $w_{\rm max}$, and $w_{\rm max}$ is fully exhausted. Figure 5 presents a demonstrative example of Algorithm 1 with N=5. In Figure 5, the algorithm first seeks to fully equalize the durations as $\tau_i = 1$, as this is the optimal pulse under no type-S degradation (Theorem 2). However, equal allocation violates a type-S lifetime since $0.5 = T_{\rm deg,1} < \tau_1 = 1$. In Step 2, the algorithm allocates $T_{\text{deg},1} = \tau_1 = 0.5$, and seeks to fully equalize all remaining $\{\tau_2,\ldots,\tau_N\}$ with the remaining energy budget. The algorithm keeps iterating until there is no type-S lifetime violation, and terminates when this condition

We now present Theorem 3, which shows that Algorithm 1 yields the optimal pulse shape for the setting considered in this subsection.

Theorem 3. Given a fixed energy budget w_{max} , Algorithm 1 yields the optimal τ vector that minimizes P_e .

2) The Case with Statistical Lifetime Information: Subsection VII-A1 assumes exact knowledge of the degradation-

induced lifetimes of the type-S molecules $T_{\text{deg},i}$, and provides the optimal pulse shape, which is not necessarily a delayedspike due to some $T_{\text{deg},i}$'s potentially constraining the allocation. The results of Subsection VII-A1 hold for any type of type-S decay profile, yet requires exact information on the type-S lifetime constraints. Similar to type-M molecule's degradation in the channel, type-S degradation is also likely to be stochastic, thus exact knowledge of $T_{\text{deg},i}$ values may not be practical. Even further, the stochastic case incurs a nonzero probability for each molecule to degrade prior to being synthesized (i.e, in cases where $\tau_i > T_{\text{deg},i}$), thus guaranteeing all molecules will be successfully converted and released before type-S degradation (i.e., Subsection VII-A1) is not feasible in practice. Motivated by this, this subsection proposes a method to deal with this stochasticity when designing the pulse shape.

The first approach we discuss herein is a natural extension taken in Subsection VII-A1 to the stochastic case. For the sake of argumentation, let us assume type-S molecules exhibit exponential decay, with rate k_S (other degradation profiles can follow an identical procedure). Assuming the transmitter has access to degradation statistics (*i.e.*, the value of k_S), it can leverage a similar approach to Subsection VII-A1 by *matching* the distribution of the decay profile as follows:

- 1) Generate N exponential random variables with rate k_S .
- 2) Sort the generated degradation times in increasing order to obtain $T_{\rm deg}$.
- 3) Run Algorithm 1 with the obtained $T_{\rm deg}$ to generate τ . On average, this approach is expected to perform worse than running Algorithm 1 with perfect information due to mismatches in degradation lifetimes. Furthermore, in cases where the generated lifetime is larger than the true $T_{{\rm deg},i}$, the algorithm is likely to lose the molecule to type-S degradation (unless Step 5 of Algorithm 1 yields a $\tau_i \leq T_{{\rm deg},i}$).

Given there is a sufficient energy budget $w_{\rm max}$, Algorithm 1 satisfies $\tau_i \leq T_{{\rm deg},i}$ for all molecules, thereby guaranteeing no type-S losses. However, when doing so, the algorithm spends a significant portion of its energy budget to a small number

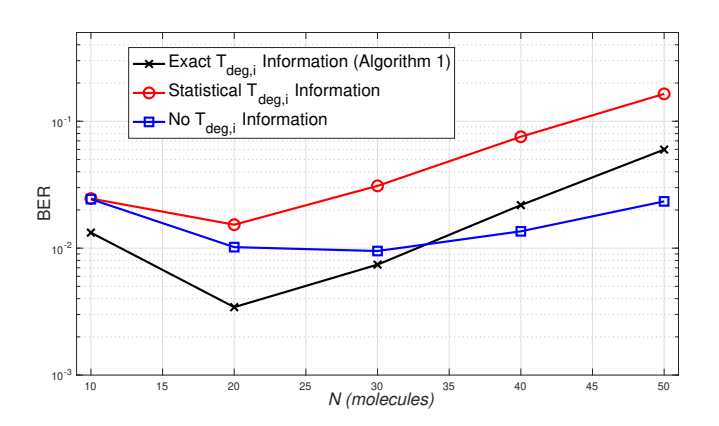


Fig. 6. BER vs. N for different methods under type-S degradation. $w(\tau)=\frac{1}{\tau},\ w_{\rm max}=10,\ d=10\,\mu{\rm m},\ D=100\,\mu{\rm m}^2\,{\rm s}^{-1},\ k=1\times 10^{-3}\,{\rm s}^{-1},\ k=5\times 10^{-2}\,{\rm s}^{-1},\ t_R=10\,{\rm s},\ \gamma=\frac{N}{2}+0.5.$ Each data point on the figure is averaged over 10^6 bit transmission realizations.

of molecules with particularly short $T_{\deg,i}$ lifetimes, leaving other molecules low remaining energy – hence larger τ_i and smaller p_i . We argue herein that avoiding this imbalance in τ_i might be desirable in some cases, even though it entails the loss of some molecules (hence transmission intensity). In particular, we herein consider invoking to Section V's result of setting $\tau_i = w^{-1}(\frac{w_{\max}}{N})$ for all i. Note that this method does not utilize any type-S degradation information, thus can be considered a no-lifetime-information method.

In order to compare the presented methods under type-S degradation, we present Figure 6. As expected, the results of Figure 6 show that running Algorithm 1 with exact $T_{\text{deg},i}$ information yields lower error probabilities than relying only on statistical information (k_S) . More importantly, the results support our claim in the previous paragraph that although Algorithm 1 is provably optimal given every type-S molecule is successfully converted and released, it may not always be the best option when type-S loss is allowed. Note that in the small N regime, every molecule's possible contribution to the received signal is significant, thus the system is better off by releasing as many molecules as possible, hence avoiding type-S losses. However, as N increases, this improvement is diminished as a single molecule's contribution is less significant. Furthermore, accommodating for a few, very constraining $T_{\text{deg},i}$ deadlines causes a large majority of the remaining molecules to increase their release times significantly in order to meet the $w_{\rm max}$ budget, thereby increasing error rates.

B. Passive (Observing) Receivers: The Non-Monotonic p_i Case

Throughout the paper, we leveraged the fact that for an absorbing receiver that cumulatively counts the arrivals, the success probability of each molecule p_i is a decreasing function of the release time \mathcal{T}_i (recall Figure 1). However, this is dependent on the particular receiver structure, and may not always hold for other receiver types such as passive (observing) receivers. Instead of absorbing, counting, and removing the molecules from the environment, passive receivers simply sample the number of molecules at a particular instant t_R , which constitute their received signal y [37].

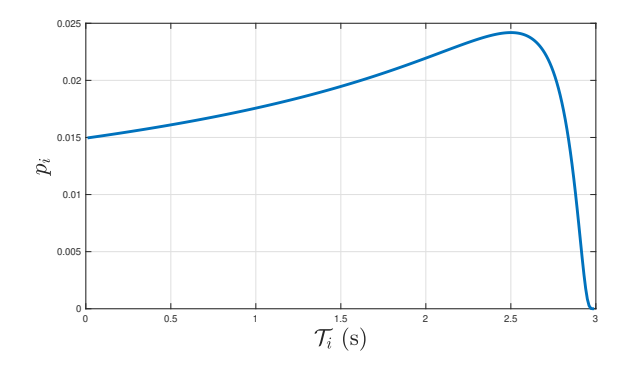


Fig. 7. Success probability p_i with respect to \mathcal{T}_i for a 1-D DBMC system with molecular degradation and a passive receiver (11). $d=10\,\mu\mathrm{m},~L=1\,\mu\mathrm{m}$ $D=100\,\mu\mathrm{m}^2\,\mathrm{s}^{-1},~k=1\times10^{-3}\,\mathrm{s}^{-1},~t_R=3\,\mathrm{s}.$

Considering a 1-D DBMC system with a point transmitter and a passive receiver that observes a region of length L, and denoting the TX/center-of-RX distance as d, a unit impulse emission from TX results in a concentration at the center point of the RX as $c(t) = \frac{1}{\sqrt{4\pi Dt}} \exp(-\frac{d^2}{4Dt})$, given no degradation in the environment [46], [47]. Considering the regime of $L \ll d$, the total concentration observed within the RX body can be approximated to be uniform across the body [37], which yields the channel impulse response

$$h_{nd}(t) = \frac{L}{\sqrt{4\pi Dt}} \exp\left(-\frac{d^2}{4Dt}\right).$$

For systems with degradation in the channel, in addition to residing in the RX observation region at $t = t_R$, a molecule released at time \mathcal{T}_i needs to survive at least until $t = t_R$ to successfully contribute to y. Considering exponential decay in the system similar to Section II, this survival probability is

$$p_{\rm surv} = P(T_{\rm surv} > t_R) = e^{-k(t_R - \mathcal{T}_i)},$$

which yields a molecule's probability of being successfully counted (that is, p_i) to be

$$p_i(\mathcal{T}_i) = \frac{L}{\sqrt{4\pi D(t_R - \mathcal{T}_i)}} \exp\left[-\frac{d^2}{4D(t_R - \mathcal{T}_i)} - k(t_R - \mathcal{T}_i)\right]. \tag{11}$$

The success probability p_i in (11) need not be monotonically decreasing in \mathcal{T}_i , as seen in Figure 7. The p_i – \mathcal{T}_i curves similar to the those in Figure 7 define scenarios where converting and releasing a molecule too early and too late are both undesirable (also see discussion in Section III on pre- and post-transmission delay constraints). We note that in such cases, the delayed-spike pulse considered previously can still be leveraged, however with a modification. Let p_i^* denote the largest success probability in the p_i – \mathcal{T}_i curve, i.e, the peak value. In cases where the equal allocation $\tau_i = \mathcal{T}_i = w^{-1}(\frac{w_{\text{max}}}{N})$ yields a common release time that is larger than $\mathcal{T}_i^{-1}(p_i^*)$ (right-hand-side of the peak), then w_{max} should be fully exhausted to minimize \mathcal{T}_i as much as possible (similar to Section V). However, if the available w_{max} allows for a common release time that is smaller than $\mathcal{T}_i^{-1}(p_i^*)$ (left-hand-side of the peak), then full utilization of w_{max} is not beneficial as a partial utilization and the resulting \mathcal{T}_i could ensure achieving the

highest success probability of p_i^* . Thus, the common release time should then be selected as

$$\mathcal{T}_i = \max\left\{w^{-1}\left(\frac{w_{\text{max}}}{N}\right), \mathcal{T}_i^{-1}(p_i^*)\right\}. \tag{12}$$

Note that for cases width multimodal $p_i(\mathcal{T}_i)$ functions (e.g., due to different degradation profiles, reaction chains that govern reception/counting at RX, etc.), this argument can be generalized.

VIII. CONCLUSIONS

In this paper, we investigated pulse shaping for DBMC, under constraints on the available energy budget for molecule transmission. Leveraging approaches from wireless packet scheduling, we developed a framework that can be used to analyze the DBMC pulse shaping problem from the perspective of energy/time allocation. Through this framework, we proved that the optimal pulse shape that minimizes BER is a delayedspike pulse under a convex energy cost on molecule synthesis duration. Numerical results show that the delayed-spike pulse outperforms conventional pulse shapes, corroborating the analysis. Building on the introduced framework, we provided extensions to cases where molecules can degrade within the transmitter before release, as well as passive/observing receiver structures. Future work includes a rigorous treatment of pulse shape design in DBMC systems with ISI, addressing the energy-constrained pulse shaping problem under different modulation schemes, and extending to non-convex energy functions.

ACKNOWLEDGEMENT

The authors gratefully acknowledge James Boedicker at the University of Southern California for their insightful comments.

APPENDIX A LEMMA 1 AND ITS PROOF

To be used in the proofs of Theorems 1-2 in Appendices B-C, we first provide a needed lemma herein.

Lemma 1. Given $\tau_i < t_R - \frac{\sqrt{9 + \frac{4kd^2}{D}} - 3}{4k}$ for all i, the error probability P_e is Schur-convex (order-preserving) in τ_i .

Proof. A function is Schur-convex if it is defined on a symmetric convex set A, is symmetric with respect to variable permutations, and it is a convex function of its variables [39], [40]. We will proceed by showing $P_e(\tau)$ satisfies all these requirements in its defined domain of interest.

Domain: The function is defined on a symmetric convex set $\sqrt{\frac{1}{2} + \frac{4kd^2}{2}}$

$$(I^N \text{ where } I = (0, t_R - \frac{\sqrt{9 + \frac{4kd^2}{D}} - 3}{4k}) \text{ for each } \tau_i).$$

Symmetry: The error probability $P_e(\tau)$ is a symmetric function on τ_i 's index permutations, that is, permuting τ_i 's do not change the value. This is a direct result of each molecule being identical and therefore contributing equally to the received signal count.

Convexity in τ_i : We will leverage the positivity of the second

derivative of P_e to prove its convexity in τ_i . Using the chain rule on the second derivative, we have

$$\frac{\partial^2 P_e}{\partial \tau_i^2} = \frac{\partial^2 P_e}{\partial p_i^2} \left(\frac{\partial p_i}{\partial \tau_i}\right)^2 + \frac{\partial P_e}{\partial p_i} \frac{\partial^2 p_i}{\partial \tau_i^2} \tag{13}$$

To evaluate $\frac{\partial^2 P_e}{\partial \tau_i^2}$, we first focus on $\frac{\partial^2 P_e}{\partial p_i^2}$. As stated in (10), that the error probability expression follows a Poisson-binomial CDF. Observe from (9) that in each summand of the error expression, which is

$$P(y=k) = \sum_{A \in \mathcal{S}_k} \prod_{i \in A} p_i \prod_{j \notin A} (1 - p_j),$$

each p_i appears exactly once (in the form of p_i or $(1-p_i)$). Therefore, each summand's second derivative with respect to p_i is zero, hence $\frac{\partial^2 P_e}{\partial \tau_i^2} = 0$. This implies the first term in (13) is always zero, and that $\frac{\partial^2 P_e}{\partial \tau_i^2} = \frac{\partial P_e}{\partial p_i} \frac{\partial^2 p_i}{\partial \tau_i^2}$. We now observe that the first subterm in the second term,

We now observe that the first subterm in the second term, $\frac{\partial P_e}{\partial p_i}$, is always negative due to the monotone decreasing nature of P_0 .

As
$$\frac{\partial P_e}{\partial p_i} < 0$$
, satisfying $\frac{\partial^2 p_i}{\partial \tau_i^2} < 0$ ensures $\frac{\partial^2 P_e}{\partial \tau_i^2} > 0$, hence convexity. We now evaluate $\frac{\partial^2 p_i}{\partial \tau_i^2} > 0$. Recalling each

hence convexity. We now evaluate $\frac{\partial^2 p_i}{\partial \tau_i^2} > 0$. Recalling each molecule's release time $\mathcal{T}_i = \tau_i$, from the fundamental theorem of calculus, we have

$$\frac{\partial p_i}{\partial \tau_i} = \left[\frac{\partial}{\partial \tau_i} \int_0^{t_R - \tau_i} f_{hit}(u) du \right] \times \frac{t_R - \tau_i}{\partial \tau_i}
= -f_{hit}(t_R - \tau_i)
= \frac{-d}{\sqrt{4\pi D(t_R - \tau_i)^3}} e^{-\frac{d^2}{4D(t_R - \tau_i)} - k(t_R - \tau_i)}.$$
(14)

Taking another derivative on this expression, we arrive at

$$\frac{\partial^2 p_i}{\partial \tau_i^2} = \frac{-d(t_R - \tau_i)e^{-\frac{d^2}{(4D - k)(t_R - \tau_i)}}}{\sqrt{4\pi} \left(4D(t_R - \tau_i)^3\right)^{\frac{3}{2}}} \times \left[4D(t_R - \tau_i)(2k(t_R - \tau_i) + 3) - 2d^2\right].$$
(15)

In (15), we first observe that the denominator is positive. Given the valid region of τ_i , $(-d)(t_R-\tau_i)$ is negative. Furthermore, $e^{(\cdot)}$ always outputs a positive number by definition. Combining these, the whole expression is negative if $\left[4D(t_R-\tau_i)(2k(t_R-\tau_i)+3)-2d^2\right]>0$ is satisfied. A reorganization yields

$$4Dku^2 + 6Du - d^2 > 0,$$

where $u=t_R-\tau_i$. This quadratic inequality has two satisfying regions: $u<\frac{-3D-\sqrt{9D^2+4kd^2}}{4Dk}$ and $u>\frac{-3D+\sqrt{9D^2+4kd^2}}{4Dk}$, where the former is invalid as it implies $\tau_i>t_R$. The latter expression is satisfied when $\tau_i< t_R-\frac{\sqrt{9+\frac{4kd^2}{D}}-3}{4k}$, which is the assumed operating regime of interest in Section V (and onwards). Thus, within the desired regime, $\frac{\partial^2 p_i}{\partial \tau_i^2}<0$, which yields $\frac{\partial^2 P_e}{\partial \tau^2}>0$, implying P_e is convex in τ_i for any i.

 6 As intuition, note that an increase in p_i implies a molecule's arrival probability is larger. All other things equal, this increase implies an increase in $P(y>\gamma|b=1)$, hence a lower error probability.

Overall, all the criteria are met for Schur-convexity, hence necessarily follows that $P_e(\tau)$ is Schur-convex (orderpreserving) in τ .

APPENDIX B PROOF OF THEOREM 1

Showing $P_e(\tau) = P_{\text{target}}$: Each τ vector induces an arrival probability p vector with $p_i = p_i(\tau_i)$, thus induces a probability of error, $P_e(\tau)$. Let τ be the energy-optimal duration, and suppose $P_e(\tau) < P_{\text{target}}$. In such a case, another vector τ' can be designed such that

- 1) For a particular $j,\, \tau_i=\tau_i'$ for all $i\neq j.$ 2) Select τ_j' such that $P_e({\pmb{\tau}}')=P_{\rm target}.$

Since $P_e(\tau)$ is monotone increasing in each τ_i , we know that $\tau'_i > \tau_j$. Combining this with $\tau_i = \tau'_i$ for all $i \neq j$, as the energy function $w(\tau)$ is decreasing in τ , we have

$$w(\tau') = \sum_{i=1}^{N} w(\tau'_i) = w(\tau'_j) + \sum_{i \neq j}^{N} w(\tau'_i)$$

$$= w(\tau'_j) + \sum_{i \neq j}^{N} w(\tau_i)$$

$$< w(\tau_j) + \sum_{i \neq j}^{N} w(\tau_i) = w(\tau),$$
(16)

implying τ cannot be energy-optimal, yielding a contradiction. Thus, any optimal τ vector to be optimal, it has to ensure $P_e(\boldsymbol{\tau}) = P_{\text{target}}.$

Showing $\tau_i = \tau_j$ for all i, j: Suppose a valid vector $\boldsymbol{\tau}$ has an arbitrary i,j pair that $\tau_i \neq \tau_j$. Then, one can set up a competitor vector $\boldsymbol{\tau}'$ with $\tau_i' = \tau_j' = \frac{\tau_i + \tau_j}{2}$, and for all other elements $\tau_l = \tau_l'$. Note that τ' gets majorized by τ . Similar to [20], as w(x) is convex decreasing in x, this new configuration yields $w(\tau') < w(\tau)$, thus τ cannot be energy-optimal.

It still remains to show is that this new allocation does not violate the error probability constraint. Note that since P_e is Schur-convex in the regime of interest (see Lemma 1 in Appendix A), the fact that au' gets majorized by au directly implies $P_e(\tau') < P_e(\tau)$. Then, given τ is valid, τ' is also valid (does not violate the error probability constraint). This argument can be recursively applied until all τ_i are equal, thus $w(oldsymbol{ au})$ is minimized if and only if $au_i = au_j$ for all $i, j \in \{1, \dots, N\}.$

Both conditions for optimality are proven, hence the proof is complete.

APPENDIX C PROOF OF THEOREM 2

We first show that the error-optimal au has to allocate all its available $w_{\rm max}$ budget. Suppose otherwise, that is, a vector au has $\sum_{i=1}^N w(au_i) < w_{\max}$, and achieves $P_e(au)$. Then, one can devise a competitor au' with $\sum_{i=1}^N w(au_i') = w_{\max}$ by decreasing the duration of a single duration, that is $\tau_i' < \tau_j$ and $\tau_i = \tau_i'$ for all $i \neq j$. Then, since as $P_e(\tau)$ is monotone increasing in each of its N arguments, we necessarily

have $P_e(\tau') < P_e(\tau)$, meaning τ cannot be optimal. Thus, $\sum_{i=1}^{N} w(\tau_i) < w_{\text{max}}$ has to hold for error-optimality.

We now show that for optimal τ , we have $\tau_i = \tau_j$ for all i, j. Suppose otherwise, that is, there exists an i, j pair such that $au_i
eq au_j$. Then, we can devise a competitor $oldsymbol{ au}'$ with $au_i' = au_j' =$ $\frac{\tau_i + \tau_j}{2}$ and $\tau_l' = \tau_l$ for all $l \neq i, j$, which gets majorized by τ , that is $\tau' \prec \tau$. Since $P_e(\tau)$ monotone increasing and Schurconvex, this necessarily implies $P_e(\tau') < P_e(\tau)$, meaning τ cannot be error-optimal. Note that similar to Appendix B, since $w(\tau)$ is Schur-convex and decreasing, we can show that $w(\tau') < w(\tau)$, thus this competitor τ' does not violate the energy budget constraint and is valid.

Overall, following both these contradictions, the energyminimizing τ vector needs to have all τ_i equal and fully exhaust the available w_{max} budget, implying $\tau_i = w^{-1}(\frac{w_{\text{max}}}{N})$ for all i. The proof is complete.

APPENDIX D PROOF OF THEOREM 3

Let a particular c be the stopping point of Algorithm 1, and let τ denote the algorithm's output. Then, by design, c is the smallest index such that $\tau_i = T_{\deg,i}$ for all $i \leq c$, the remaining durations $\tau_{c+1} = \cdots = \tau_N = \frac{w_{\max} - \sum_{i=1}^c w(T_{\deg,i})}{N-c} > T_{\deg,c}$, and $\sum_{i=1}^{N} w(\tau_i) = w_{\text{max}}$.

Given an energy budget w_{max} , we first show that the optimal vector has to have $\tau_i = T_{\text{deg},i}$ for all $i \leq c$. Suppose by contradiction that a competitor vector au' has $au_i = T_{\deg,i} - \epsilon$ for some $\epsilon > 0$ at an arbitrary index $i \leq c$, and $\tau'_i = T_{\text{deg},j}$ for the rest of indices $j \leq c$, $j \neq i$. As $w(\tau)$ is decreasing, $w(\tau_i') > w(T_{\text{deg},i})$ is true, meaning the remaining N-1molecules of τ' with index $j \neq i$ have less energy budget to allocate compared to their counterparts in τ . Thus, at least one element of τ' should be larger than its same-index counterpart in τ . Clearly, the larger duration(s) cannot be selected from indices $\{1,\ldots,i-1,i+1,\ldots,c\}$, as they are already at their maximum allowable values due to their $T_{{
m deg},i}$ limits. Then the remaining N-c durations of τ' should be set $\tau'_{c+1} = \cdots = \tau'_N = \frac{w_{\max} - \sum_{i=1}^c w(\tau'_i)}{N-c}$, since this is the best allocation inter terms of P_e as it exhausts all remaining energy left to $\{\tau'_{c+1}, \dots, \tau'_{N}\}$ and has all equal durations among them (follows identical to Theorem 2) 8. Note that this is equivalent to having $\tau_i' = \tau_i + \delta$ for some $\delta > 0$ as $\tau_{c+1} = \cdots = \tau_N$. Due to the convex and decreasing nature of $w(\tau)$, we necessarily have $\delta > \frac{\epsilon}{N-c}$ to still satisfy $\sum_{i=1}^N w(\tau_i') = w_{\max}$. Let another vector $\boldsymbol{\tau}''$ be such that $\delta = \frac{\epsilon}{M-c}$ for these elements, and for the remaining elements $\boldsymbol{\tau}' = \boldsymbol{\tau}''$. Clearly, $P_e(\boldsymbol{\tau}'') < P_e(\boldsymbol{\tau}')$. Also observe that we necessarily have $\sum_{i=1}^N \tau_i = \sum_{i=1}^N \tau_i''$ for this

⁷This argument can be directly generalized to multiple such indices by considering each index one-by-one.

⁸We assume this allocation does not violate type-S deadlines of molecules $\{c+1,\ldots,N\}$ for clarity of presentation. In case it does violate for indices $\{c+1,\ldots,c+g\}$, arranging $\tau'_{c+1},\ldots,\tau'_N$ with the energy budget $w_{\max}-\sum_{i=1}^c w(\tau'_i)$ yields a subproblem that is identical in nature to the original problem we prove herein. The optimal allocation of this subproblem would be allocating $\{c+1,\ldots,c+g\}$ critically and $\{c+g+1,\ldots,N\}$ equally with the remaining energy, with a proof that is identical to the one laid out in this appendix. This can be recursively done until there is no violations at this step in the proof.

third vector, and that τ'' majorizes τ summing up to the same value. This implies $P_e(\tau) < P_e(\tau'')$ due to Schur-convexity of P_e , hence $P_e(\tau) < P_e(\tau')$, implying the competitor vector τ' cannot be optimal. Thus, $\tau_i = T_{\deg,i}$ for all $i \leq c$ has to be true. Lastly, given $\tau_i = T_{\deg,i}$ for all $i \leq c$, fully exhausting the remaining energy $w_{\max} - \sum_{i=1}^c w(T_{\deg,i})$ and allocating among $\{\tau_{c+1}, \ldots, \tau_N\}$ is optimal to minimize a Schur-convex P_e , which concludes the proof.

REFERENCES

- M. C. Gursoy, M. Nasiri-Kenari, and U. Mitra, "Towards high datarate diffusive molecular communications: A review on performance enhancement strategies," *Digital Signal Processing*, p. 103161, May 2022.
- [2] N. Garralda, I. Llatser, A. Cabellos-Aparicio, E. Alarcón, and M. Pierobon, "Diffusion-based physical channel identification in molecular nanonetworks," *Nano Communication Networks*, vol. 2, no. 4, pp. 196– 204. Dec. 2011.
- [3] B. Dhayabaran, G. T. Raja, M. Magarini, and H. B. Yilmaz, "Transmit signal shaping for molecular communication," *IEEE Wireless Commu*nications Letters, vol. 10, no. 7, pp. 1459–1463, Jul. 2021.
- [4] B. Tepekule, A. E. Pusane, M. S. Kuran, and T. Tugcu, "A novel pre-equalization method for molecular communication via diffusion in nanonetworks," *IEEE Communications Letters*, vol. 19, no. 8, pp. 1311– 1314. Jun. 2015.
- [5] W. Wicke, R. C. Felsheim, L. Brand, V. Jamali, H. M. Loos, A. Buettner, and R. Schober, "Pulse shaping for MC via particle size," *IEEE Transactions on Molecular, Biological and Multi-Scale Communications*, pp. 1–1, Mar. 2023.
- [6] S. Wang, W. Guo, and M. D. McDonnell, "Transmit pulse shaping for molecular communications," in *IEEE Conference on Computer Communications Workshops*, Apr. 2014, pp. 209–210.
- [7] M. C. Gursoy, H. B. Yilmaz, A. E. Pusane, and T. Tugcu, "Simulation study and analysis of diffusive molecular communications with an apertured plane," *IEEE Transactions on NanoBioscience*, vol. 19, no. 3, pp. 468–476, Jul. 2020.
- [8] H. Yan, G. Chang, Z. Ma, and L. Lin, "Derivative-based signal detection for high data rate molecular communication system," *IEEE Communi*cations Letters., vol. 22, no. 9, pp. 1782–1785, Sep. 2018.
- [9] M. C. Gursoy and U. Mitra, "Higher order derivative-based receiver preprocessing for molecular communications," *IEEE Transactions on Molecular, Biological and Multi-Scale Communications*, vol. 8, no. 3, pp. 178–189, Feb. 2022.
- [10] M. Movahednasab, M. Soleimanifar, A. Gohari, M. Nasiri-Kenari, and U. Mitra, "Adaptive transmission rate with a fixed threshold decoder for diffusion-based molecular communication," *IEEE Transactions on Communications*, vol. 64, no. 1, pp. 236–248, Jan. 2016.
- [11] T. N. Cao, A. Ahmadzadeh, V. Jamali, W. Wicke, P. L. Yeoh, J. Evans, and R. Schober, "Diffusive mobile mc with absorbing receivers: Stochastic analysis and applications," *IEEE Transactions on Molecular, Biological and Multi-Scale Communications*, vol. 5, no. 2, pp. 84–99, Nov. 2019.
- [12] M. K. Zadeh, I. M. Bolhassan, and M. Kuscu, "Microfluidic pulse shaping methods for molecular communications," *Nano Communication Networks*, p. 100453, Jun. 2023.
- [13] N. Farsad, H. B. Yilmaz, A. Eckford, C. Chae, and W. Guo, "A comprehensive survey of recent advancements in molecular communication," *IEEE Communications Surveys & Tutorials*, vol. 18, no. 3, pp. 1887–1919, Thirdquarter 2016.
- [14] J. Shaska, M. C. Gursoy, T. D. Ross, Y.-Y. Cheng, A. Krieger, M. Thairu, O. Venturelli, J. Boedicker, J. Handelsman, and U. Mitra, "Microbes as communication and decision-making networked communities," to appear in IEEE Nanotechnology Magazine, May 2023.
- [15] M. Tei, M. L. Perkins, J. Hsia, M. Arcak, and A. P. Arkin, "Designing spatially distributed gene regulatory networks to elicit contrasting patterns," ACS Synthetic Biology, vol. 8, no. 1, pp. 119–126, Dec. 2018.
- [16] S. Gupta, "Manipulating spatiotemporal variables to program coordinated behaviors in microbial consortia," Ph.D. dissertation, University of Wisconsin-Madison, 2021.
- [17] S. Gupta, T. D. Ross, M. M. Gomez, J. L. Grant, P. A. Romero, and O. S. Venturelli, "Investigating the dynamics of microbial consortia in spatially structured environments," *Nature Communications*, vol. 11, no. 1, pp. 1–15, May 2020.

- [18] J. K. Kim, Y. Chen, A. J. Hirning, R. N. Alnahhas, K. Josić, and M. R. Bennett, "Long-range temporal coordination of gene expression in synthetic microbial consortia," *Nature chemical biology*, vol. 15, no. 11, pp. 1102–1109, Oct. 2019.
- [19] T. I. Yusufaly and J. Q. Boedicker, "Spatial dispersal of bacterial colonies induces a dynamical transition from local to global quorum sensing," *Physical Review E*, vol. 94, no. 6, p. 062410, 2016.
- [20] E. Uysal-Biyikoglu, B. Prabhakar, and A. El Gamal, "Energy-efficient packet transmission over a wireless link," *IEEE/ACM Transactions on Networks*, vol. 10, no. 4, pp. 487–499, Aug. 2002.
- [21] W. Chen, M. J. Neely, and U. Mitra, "Energy-efficient transmissions with individual packet delay constraints," *IEEE Transactions on Information Theory*, vol. 54, no. 5, pp. 2090–2109, May 2008.
- [22] M. C. Gursoy and U. Mitra, "Energy-efficient packet scheduling under two-sided delay constraints," in *IEEE International Conference on Communications (ICC)*, May 2023.
- [23] ——, "Two-sided delay constrained scheduling: Managing fresh and stale data," *IEEE Transactions on Wireless Communications*, pp. 1–1, Aug. 2023.
- [24] A. C. Heren, H. B. Yilmaz, C.-B. Chae, and T. Tugeu, "Effect of degradation in molecular communication: Impairment or enhancement?" *IEEE Transactions on Molecular, Biological and Multi-Scale Commu*nications, vol. 1, no. 2, pp. 217–229, Nov. 2015.
- [25] A. Noel, K. C. Cheung, and R. Schober, "Improving receiver performance of diffusive molecular communication with enzymes," *IEEE Transactions on NanoBioscience*, vol. 13, no. 1, pp. 31–43, Mar. 2014.
- [26] M. S. Kuran, H. B. Yilmaz, I. Demirkol, N. Farsad, and A. Goldsmith, "A survey on modulation techniques in molecular communication via diffusion," *IEEE Communications Surveys & Tutorials*, vol. 23, no. 1, pp. 7–28, Firstquarter 2021.
- [27] B. Koo, C. Lee, H. B. Yilmaz, N. Farsad, A. Eckford, and C. Chae, "Molecular MIMO: From theory to prototype," *IEEE Journal on Selected Areas in Communications*, vol. 34, no. 3, pp. 600–614, Mar. 2016.
- [28] M. Damrath and P. A. Hoeher, "Low-complexity adaptive threshold detection for molecular communication," *IEEE Transactions on NanoBioscience*, vol. 15, no. 3, pp. 200–208, Apr. 2016.
- [29] T. N. Cao, V. Jamali, N. Zlatanov, P. L. Yeoh, J. Evans, and R. Schober, "Fractionally spaced equalization and decision feedback sequence detection for diffusive MC," *IEEE Communications Letters*, vol. 25, no. 1, pp. 117–121, Jan. 2021.
- [30] J. M. Schmiedel, L. B. Carey, and B. Lehner, "Empirical mean-noise fitness landscapes reveal the fitness impact of gene expression noise," *Nature Communications*, vol. 10, no. 1, p. 3180, Jul. 2019.
- [31] M. Scott, C. W. Gunderson, E. M. Mateescu, Z. Zhang, and T. Hwa, "Interdependence of cell growth and gene expression: origins and consequences," *Science*, vol. 330, no. 6007, pp. 1099–1102, Nov. 2010.
- [32] H. Dong, L. Nilsson, and C. G. Kurland, "Gratuitous overexpression of genes in escherichia coli leads to growth inhibition and ribosome destruction," *Journal of bacteriology*, vol. 177, no. 6, pp. 1497–1504, Mar. 1995.
- [33] D. A. F. Fuentes, P. Manfredi, U. Jenal, and M. Zampieri, "Pareto optimality between growth-rate and lag-time couples metabolic noise to phenotypic heterogeneity in escherichia coli," *Nature communications*, vol. 12, no. 1, p. 3204, May 2021.
- [34] X. Huang, Y. Fang, A. Noel, and N. Yang, "Channel characterization for 1-D molecular communication with two absorbing receivers," *IEEE Communications Letters*, vol. 24, no. 6, pp. 1150–1154, Jun. 2020.
- [35] B. Tepekule, A. E. Pusane, H. B. Yilmaz, C.-B. Chae, and T. Tugcu, "ISI mitigation techniques in molecular communication," *IEEE Transactions on Molecular, Biological, and Multi-Scale Communications*, vol. 1, no. 2, pp. 202–216, Jun. 2015.
- [36] H. Arjmandi, M. Movahednasab, A. Gohari, M. Mirmohseni, M. Nasiri-Kenari, and F. Fekri, "ISI-avoiding modulation for diffusion-based molecular communication," *IEEE Transactions on Molecular, Biological, and Multi-Scale Communications*, vol. 3, no. 1, pp. 48–59, Dec. 2016.
- [37] V. Jamali, A. Ahmadzadeh, W. Wicke, A. Noel, and R. Schober, "Channel modeling for diffusive molecular communication—a tutorial review," *Proceedings of the IEEE*, vol. 107, no. 7, pp. 1256–1301, Jun. 2019.
- [38] K. V. Srinivas, A. W. Eckford, and R. S. Adve, "Molecular communication in fluid media: The additive inverse gaussian noise channel," *IEEE Transactions on Information Theory*, vol. 58, no. 7, pp. 4678–4692, Jul. 2012.
- [39] A. W. Marshall and I. Olkin, "Inequalities via majorization—an introduction," in *General Inequalities 3*. Springer, 1983, pp. 165–187.

- [40] C. law St, "An effective characterization of Schur-convex functions with applications," *Journal of Convex Analysis*, vol. 14, no. 1, pp. 103–108, 2007.
- [41] J. Yang and S. Ulukus, "Optimal packet scheduling in an energy harvesting communication system," *IEEE Transactions on Communications*, vol. 60, no. 1, pp. 220–230, Jan. 2011.
- [42] X. Kang, C. K. Ho, and S. Sun, "Full-duplex wireless-powered communication network with energy causality," *IEEE Transactions on Wireless Communications*, vol. 14, no. 10, pp. 5539–5551, Oct. 2015.
- [43] D. Bertsekas and R. Gallager, Data networks. Athena Scientific, 2021.
- [44] S. Tsitkov, T. Pesenti, H. Palacci, J. Blanchet, and H. Hess, "Queueing theory-based perspective of the kinetics of "channeled" enzyme cascade reactions," ACS Catalysis, vol. 8, no. 11, pp. 10721–10731, Oct. 2018.
- [45] J. Peccoud and B. Ycart, "Markovian modeling of gene-product synthesis," *Theoretical Population Biology*, vol. 48, no. 2, pp. 222–234, Oct. 1995.
- [46] A. Einstein, Investigations on the Theory of the Brownian Movement. Courier Corporation, 1956.
- [47] L.-S. Meng, P.-C. Yeh, K.-C. Chen, and I. F. Akyildiz, "On receiver design for diffusion-based molecular communication," *IEEE Transactions on Signal Processing*, vol. 62, no. 22, pp. 6032–6044, Sep. 2014.



Mustafa Can Gursoy received the B.S. and M.S. degrees in electrical and electronics engineering from Bogazici University, Istanbul, Turkey, in 2015 and 2018, respectively. He received his Ph.D. in 2023 from the University of Southern California, Los Angeles, USA. His research interests include transceiver design, channel modeling, and networking approaches for molecular and next-generation wireless communications.

Urbashi Mitra received the B.S. and the M.S. degrees from the University of California at Berkeley and her Ph.D. from Princeton University. She is currently the Gordon S. Marshall Professor in Engineering at the University of Southern California with appointments in Electrical Engineering and Computer Science. She is the inaugural Editor-in-Chief for the IEEE Transactions on Molecular, Biological and Multi-scale Communications. She was a member of the IEEE Information Theory Society's Board of Governors (2002-2007, 2012-2017), the IEEE Signal Processing Society's Technical Committee on Signal Processing for Communications and Networks (2012-2017), the IEEE Signal Processing Society's Awards Board (2017-2018), and the Vice Chair of the IEEE Communications Society, Communication Theory Working Group (2017-2018). Dr. Mitra is a Fellow of the IEEE. She is the recipient of: the 2021 Viterbi School of Engineering Senior Research Award, the 2017 IEEE Communications Society Women in Communications Engineering Technical Achievement Award, a 2016 UK Royal Academy of Engineering Distinguished Visiting Professorship, a 2016 US Fulbright Scholar Award, a 2016-2017 UK Leverhulme Trust Visiting Professorship, 2015-2016 IEEE Communications Society Distinguished Lecturer, 2012 Globecom Signal Processing for Communications Symposium Best Paper Award, 2012 US National Academy of Engineering Lillian Gilbreth Lectureship, the 2009 DCOSS Applications & Systems Best Paper Award, Texas Instruments Visiting Professor (Fall 2002, Rice University), 2001 Okawa Foundation Award, 2000 OSU College of Engineering Lumley Award for Research, 1997 OSU College of Engineering MacQuigg Award for Teaching, and a 1996 National Science Foundation CAREER Award. Her research interests are in: wireless communications, communication and sensor networks, biological communication systems, detection and estimation and the interface of communication, sensing and control.